

# Structure–property relationships of flexible polyurethane foams

Dimitrios V. Dounis and Garth L. Wilkes\*

Department of Chemical Engineering, Polymer Materials and Interfaces Laboratory, Virginia Polytechnic Institute and State University, Blacksburg, VA 24061-0211, USA  
 (Received 11 July 1996)

In this study the viscoelastic and compression set properties were studied as a function of temperature and humidity for a series of moulded foams based on toluene diisocyanate (TDI) and glycerol initiated ethylene-oxide-capped propylene-oxide. The results were compared to those obtained on conventional slabstock foams based on TDI and glycerol initiated propylene-oxide. These comparisons were made to delineate and clarify distinct differences between these two different but very important systems. It was found that high temperatures and humidities 'plasticized' the moulded foams to a greater extent than the slabstock foams. Moulded foams displayed a higher compression set value and higher load decay value in the viscoelastic measurements than slabstock foams. In an attempt to understand these dramatic differences, the two types of 'cross-links' (covalent cross-links and urea-based phase separated hard segment domains) were more directly compared. It was found that the hard segment domains in the slabstock foam had a much higher level of short range ordering and cohesiveness. This was first confirmed by comparing the wide-angle X-ray scattering (WAXS) patterns where the amorphous character was much more pronounced in the moulded systems of equal water/TDI content. The WAXS behaviour of the slabstock system distinctly displayed short range ordering of the TDI based units. Second, Fourier transform infrared (FTi.r.) data from the carbonyl region showed that the slabstock foam had a much higher level of bidentate urea (strong hydrogen bonding) within the hard segments. Conversely, the moulded foam displayed no bidentate urea but only monodentate urea or weaker hydrogen bonding within the hard segments. This is not to imply that microphase separation did not occur since small angle X-ray scattering (SAXS) clearly showed evidence of a phase separated morphology for both types of foam systems. It is thus concluded that the dramatic differences between the mechanical properties of moulded and slabstock foams are due in part to differences in the covalent network but mostly due to the lower and weaker ordering of the hard segments in moulded systems making these physical cross-links more labile at higher temperatures and humidities. These morphological differences are believed to be due primarily to two differences in the formulation components and processing between the two studied systems. First, the ethylene-oxide capping used in the polyol of moulded foams to increase the reactivity is known to also increase the compatibility between the hard and soft segments. Second, the addition of diethanolamine (DEOA) added in the moulded foam formulation to decrease demould times by enhancing more rapid cross-linking has been shown to prevent the full local packing development of the hard-segment domains (physical cross-links). © 1997 Elsevier Science Ltd.

(Keywords: polyurethane foam; slabstock foam; moulded foam; viscoelastic; compression set; morphology; structure–property behaviour)

## INTRODUCTION

Polyurethane foams are used in a very wide range of applications primarily in the areas of insulation, packaging and load-bearing such as cushioning. Moulded foams comprise an increasing fraction of polyurethane foams because they possess many advantages over slabstock foams—the greatest being that the foam can be moulded into the desired intricate shape, thus eliminating the need for labour-intensive cutting and waste. Also, moulded foams can be produced with multiple zones of hardness, with reinforcements, or with a liner such as plastic or fabric skin which reduce labour costs of final product assembly. In view of this trend, the need exists for a greater fundamental understanding of the relationships between the structure/morphology and physical properties of these two types of polyurethane

foams. For example, the network structure of a typical polyurethane foam is comprised of both chemical and physical 'cross-links'. The chemical cross-links arise from the use of a hydroxyl polyol of functionality greater than two while the physical 'cross-links' arise from the phase separated hard segment domains (urea segments). Although both types of 'cross-links' enhance the foams physical properties, the physical 'cross-links' are liable at high temperatures and high humidity thus dramatically altering the foams properties. This paper correlates the mechanical behaviour of moulded polyurethane foams to the morphology and chemistry through an analysis of the temperature/humidity influence on the load relaxation behaviour as well as through an investigation of other structure–property relationships. In addition, qualitative comparisons are made to previous work out of this laboratory on conventional slabstock foams specifically performed by Moreland *et al.*<sup>1</sup>.

\* To whom correspondence should be addressed

The effects of temperature and humidity on certain physical properties of polyurethane foams have been studied and well documented<sup>1-4</sup>. For example, Moreland, *et al.* of this same laboratory investigated the effects of temperature and humidity on the load relaxation and creep behaviour of slabstock polyurethane foams. Specific results from that study will be utilized here for purposes of comparison. In short, they found that an increase in temperature both 'plasticized' the hydrogen bonds between the urea segments and promoted increases in the exhibited force (rubber elasticity effect) in view of the covalent network. In the stress relaxation measurements, an increase in stress was observed with increases in temperature (up to *ca.* 100°C) for a low water content foam. In a high water content foam, no change in stress was observed with temperature (up to *ca.* 100°C), which was attributed to the higher HS content providing more hydrogen bonding available for disruption by temperature and humidity and less soft segment content to promote the 'rubber elasticity' effect. The overall result of this was a balancing of the rubber elasticity effect by the 'plasticization' due to increased temperature. Increasing the humidity also 'plasticized' the behaviour allowing for more chain slippage and thus low stress values and increased stress decays. As with temperature, the effect was more pronounced with the higher HS foams.

Herrington and Klarfeld also reported a similar trend with temperature and humidity on the compression set behaviour of slabstock foams which is a measure of the loss of thickness of a foam following compression at a specified environmental condition for a specified length of time<sup>2</sup>. They found that increased temperature and humidity resulted in increased compression set or greater thickness loss. The effects were more pronounced in the higher HS content foams and were attributed to a 'plasticization' by temperature or water which disrupt hydrogen bonds between urea segments. Patten and Seefried also observed similar trends with temperature and humidity as well as water content on compression set<sup>3</sup>.

Skorpenske *et al.* noted distinct decreases in specific properties such as tensile properties and dynamic mechanical properties with increases in temperature in slabstock flexible polyurethane foams<sup>4</sup>. In addition, the amount of compression set also increased with increasing test temperature. More importantly, when high humidity was included, the compression set was even more severe and maximum levels were attained at higher temperatures. This effect was further accentuated as the hard segment content was increased. The observed behaviour was attributed to stress yielding of the hard domains and hydrogen bond disruption.

Thomas *et al.* studied the effect of increasing the cross-link density on the morphology of flexible moulded polyurethane foams<sup>5</sup>. They altered the level of cross-linking by changing the functionality of the polyol (2.56–2.76) which was accomplished by the addition of monofunctional polyether molecules. Both SAXS and thermal analysis suggested that increasing the polyol functionality increased the phase mixing. The authors added that the morphology was the primary determining factor as to how these materials responded to varying environmental conditions.

A comparison between moulded foams and slabstock foams has recently been reported by McClusky *et al.*<sup>6</sup>.

They found that the development of urea hydrogen bonding was much more distinct in slabstock foams over moulded foams observed with FTIR. The viscosity profiles were also very different where initial viscosity build was attributed to the development of bidentate urea hard segments in the slabstock foam. In the moulded foam, an increase in viscosity was observed only at the onset of the covalent gel and did not show evidence of bidentate urea formation. These differences were attributed to the addition of DEOA and ethylene oxide capping of the polyol. Interestingly, SAXS suggested a stronger microphase separation for the moulded foams over the slabstock foam. The results of this later report will be further substantiated in this paper where additional characterization methods have also been applied to systematically prepared foams of known chemistry.

## EXPERIMENTAL

### Materials

The samples of flexible water-blown moulded polyurethane foams were made with a Hi-Tech RCM 30 foam machine at Dow Chemical in Freeport, Texas. This operation consists of two hydraulic pistons to dispense the liquid components to the mixing head. The formulation components presented in Table 1 were prepared in two storage tanks, A and B. The A side consisted of the isocyanate. The B side consisted of the polyols, water, surfactants, and catalysts. An aluminium mould having dimensions of 15" × 15" × 4.5" was used. This mould was heated to 140°F (60°C) at which point the foam mixture was dispensed into the mould. The mould was placed in an oven at 250°F (121°C) for 2.5 min after which the foam pad was removed and mechanically crushed by passing it three times through steel rollers while decreasing the gap.

The samples of the flexible water-blown slabstock foams were also made at Dow Chemical in a box-foaming operation and whose components are also shown in Table 1. Here the B-side components were first mixed for 30 s using an 8 hp electric mixer at 1800 rpm. The isocyanate was then added and the components were mixed for 5 s at 1800 rpm at which

Table 1 Formulation components of the foams studied

Component	Mould		Slabstock			Component
	Fm2	Fm4	Fs2	Fs4	Fs5	
V4703	50	50	100	100	100	V3100
CPP	50	50				
H <sub>2</sub> O	4	2	2	4	5	H <sub>2</sub> O
DEOA	1.6	1.6				
Y-10515	1.08	1.08	1.0	1.0	1.0	BF-2370
DC-5244	0.54	0.54				
DABCO 33LV	0.43	0.43	0.3	0.3	0.3	DABCO 33LV
NIAX A107	0.32	0.32				
NIAX A4	0.32	0.32	0.15	0.15	0.15	T-9
TDI	28.32	47.68	30.79	52.06	62.70	TDI
Density (lb ft <sup>-3</sup> )	3.3	1.9	2.85	1.43	1.24	Density (lb ft <sup>-3</sup> )

All formulation amounts are given as parts per hundred of polyol, pphp. Description of components: V4703: 5000 molecular weight ethylene-oxide capped triol; V3100: 3000 molecular weight triol; CPP: copolymer polyol; DEOA: cross-linking agent; Y10515, DC-5244, BF-2370: T-9 surfactants; DABCO 33LV, NIAX A107, NIAX A4: gel, blow, and cure catalysts; TDI: 80/20 blend of 2,4- and 2,6-toluene diisocyanate

point they were poured into an open box having dimensions of 15" × 15" × 12" and allowed to cure. The samples here being experimental materials are much smaller in size and inherently undergo different thermal histories than commercial foams. Temperature profiles of typical slabstock foams of different sizes are well illustrated in a treatise on antioxidant effects for foams by Skorpenske *et al.*<sup>7</sup>.

As can be seen in *Table 1*, a greater number of components were used in the formulation of moulded foams than for slabstock foams. In addition, the components differ significantly in chemistry and structure. For example, in the slabstock formulation, the polyol used was a 3000 molecular weight polyether triol—typical of conventional commercial slabstock systems. The polyol used in the moulded foams was a commonly employed 5000 molecular weight ethylene oxide capped polyether triol. The ethylene oxide capping was used in view of its much higher reactivity (due to the primary hydroxyl groups) over propylene oxide to allow for low demould times—one of the principle objectives for the development of moulded foams. Another major difference between the formulation components of moulded foams and the slabstock foams was the inclusion of styrene/acrylonitrile based copolymer (CPP) particulates of *ca.* 0.5 μm in diameter which become dispersed throughout the final foam matrix. These CPP particulates are added as a dispersion within the base polyol to aid in cell opening and act as a reinforcer. The final *major difference is the addition of DEOA in the moulded foam* formulation which is a cross-linker added to allow the foam to set in a shorter amount of time again decreasing demould times.

The basic reactions involved in the production of polyurethanes are often referred to as the blowing and gelling reactions. The reaction products of the blowing reaction between the TDI and water are carbon dioxide which foams the reacting mixture and a disubstituted amine. The amine produced in this reaction reacts with additional isocyanate to produce rigid urea groups which when of sufficient size and concentration, phase separate into urea rich domains (hard segment domains) primarily due to hydrogen bonding with additional urea groups. *Figure 1* illustrates the three basic levels of structure of increasing magnification that are typically found in moulded foams with simplified diagrams beginning with the cellular structure. An enlargement of a cell strut would reveal the solid morphology depicted in the second diagram in *Figure 1*. This illustrates a three-phase model showing the soft phase, the large CPP particulates and the hard segment (HS) domains. The model unrealistically neglects imperfections in the hard segment domains as well as single urea segments not found in domains but rather mixed in the soft phase or interfacial region. Also not shown are possible 'urea aggregates' that can sometimes form in higher hard segment containing foams. The HS domains are commonly referred to as physical 'cross-links' since they enhance the physical properties at room temperature and low humidity. At elevated temperatures and humidities, these physical 'cross-links' are significantly labile thereby altering the properties of the foams. The hard-segment domains (structure, order, concentration) play a very important role on the final structure, morphology, and properties of the foam. The reaction product between the isocyanate and multifunctional polyol is a urethane

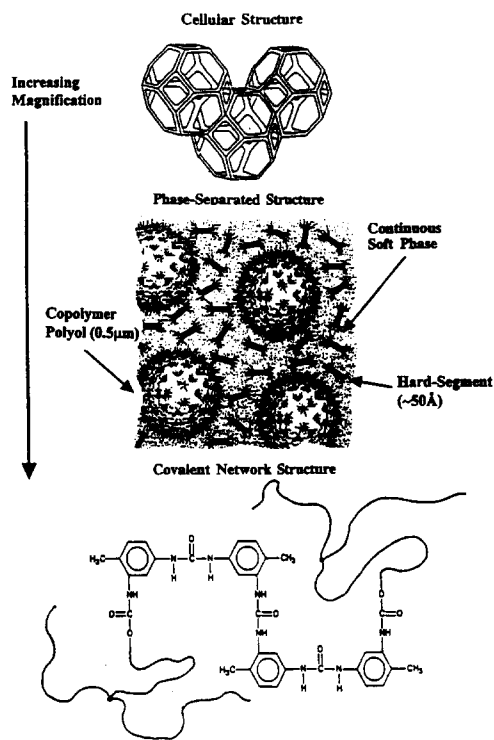


**Figure 1** Simplified diagram of the different levels of structure in moulded polyurethane foams increasing in magnification (from ref. 12)

group which links the urea groups to the ether soft segments and provides for a covalently cross-linked network as illustrated in the lower most portion of *Figure 1* of even higher magnification schematically showing the cross-linked polymer chains.

#### Experimental methods

The cellular structure of these foams was evaluated and compared using scanning electron microscopy (SEM). Thin slices (3–4 mm) of foam were adhered to aluminium stubs using silver paint and allowed to dry. A thin layer of gold was then applied to the surface of the foam using a SPI model 13131 sputter coater. Micrographs were taken using a Cambridge Stereoscan 100 SEM operating at 20 kV at a magnification of approximately 30 ×.

The procedure used for the compression set experiments was a non-ASTM procedure but was designed to reflect the load relaxation measurements. The samples were cut into dimensions of 2 × 2 × 1 inch and dried under vacuum for approximately 3.5 h. They were then placed in the environmental chamber at the designated environmental conditions for *ca.* 1 h following which they were compressed to 65% for 3 h. The samples were then removed and placed in an oven equilibrated at 40°C for 30 min after which thickness measurements were made. Recovery measurements were carried out on the samples which displayed the greatest amount of compression set (100°C–98% RH). After about one month of room temperature storage, these samples were placed in an oven at 100°C for 1 h. The thickness of the foams was again measured and recorded.

Compression load–strain measurements were conducted using the identical experimental setup used in the load relaxation measurements (described later). The 3.5" × 3.5" × 1" samples were first dried under vacuum and at 40°C for 3.5 h and placed in an environmental chamber at 30°C–35%RH for *ca.* 60 min. The samples

were then compressed at  $350 \text{ mm min}^{-1}$  to 75% strain and released. This was done to compare the level of hysteresis as a function of water content used in the formulation. By numerical integration, the energies upon loading and unloading were calculated leading subsequently to the fractional hysteresis,  $1 - E_u/E_l$ , where  $E_u$  is the energy upon unloading and  $E_l$  is the energy upon loading.

Load relaxation experiments were performed using a similar procedure as that used and described by Moreland which was originally designed to mimic the ASTM procedure used for ILD testing<sup>1</sup>. Samples, having dimensions of  $3.5'' \times 3.5'' \times 1''$ , were cut from the foam bun using a band saw equipped with a smooth 'wavy edge' saw blade. Each sample was first dried under vacuum and at  $40^\circ\text{C}$  for 3.5 h in order to give each sample an equal level of moisture. The samples were then placed in an environmental chamber preset at the testing conditions for *ca.* 60 min. The environmental chamber was purchased from Russells Technical Products and was equipped with a Watlow 922 microprocessor which controls temperature in the range of  $20^\circ\text{C}$  to  $300^\circ\text{C}$  and humidity in the range of 0 to 100%. The chamber was fit into the Instron frame equipped with a model MDB-10 compression load cell manufactured by Transducer Techniques. Using a 2'' indenter, initially at rest, the samples were twice compressed to 70% and released at a rate of  $350 \text{ mm min}^{-1}$ . After 5 min the samples were compressed to 65% strain at which point the load was immediately monitored via computer. At 65% compression, relaxation is believed to occur predominantly within the solid polymer independent of cellular structure since the onset of 'densification' is observed here.

Extraction experiments were carried out on selected samples to compare the level of cross-linking between the moulded foams and slabstock foam. Samples ( $<0.15 \text{ g}$ ) were cut from the centre of the foam bun, dried and weighed. The samples were submerged in DMF of approximately  $10 \times$  the foam volume for a period of 48 h and then taken out, dried under vacuum and at  $40^\circ\text{C}$  for approximately 24 h, following which the temperature was raised to  $80^\circ\text{C}$  for an additional 48 h. The samples were then weighed again.

In studying the degree of order within the hard segment domains, WAXS patterns were obtained. The X-ray source was a Philips X-ray generator model PW1720 using a Statton camera and a fine focus tube with nickel filtered  $\text{CuK}_\alpha$  radiation having a wavelength of  $1.542 \text{ \AA}$ . Foam samples were cut approximately 10 mm thick and compressed to approximately 3 mm. The sample-to-film distance was 8 cm and all exposure times were 10 h.

FTi.r. was used to compare the relative degree of order of the hard segments of the moulded foams and slabstock foam on a Digilab FTS-40 spectrophotometer equipped with an attenuated total reflectance (ATR) cell. For each sample 64 scans were averaged taken in the range of  $400 \text{ cm}^{-1}$  to  $4000 \text{ cm}^{-1}$  with a resolution of  $4 \text{ cm}^{-1}$ . All scans were normalized to the absorbance of a CH stretch at  $2945 \text{ cm}^{-1}$ . The regions studied were: the amide I region ( $1620\text{--}1800 \text{ cm}^{-1}$ ), the N-H region ( $3100\text{--}3500 \text{ cm}^{-1}$ ), and the isocyanate region ( $2200\text{--}2400 \text{ cm}^{-1}$ ).

Phase separation was in part evaluated using SAXS scans which were obtained with a Phillips model PW1729 generator operating at 40 kV and 20 mA. The smeared

data were collected using a Kratky camera, with nickel filtered  $\text{CuK}_\alpha$  radiation having a wavelength of  $1.542 \text{ \AA}$  passing through a slit collimator ( $0.03 \times 5 \text{ mm}$ ). The detector used is a Braun OED 50 position-sensitive platinum wire detector. The raw data were corrected for parasitic scattering and normalized using a Lupolen standard. The foam samples were cut approximately 10 mm thick and compressed to approximately 3 mm.

## RESULTS AND DISCUSSION

### Cellular structure and solid morphology

The cellular structure of the moulded foams was compared to the cellular structure of the slabstock foams. Figure 2 shows two micrographs of the 4pph water content slabstock foam (Fs4), parallel and perpendicular to the rise direction. As can be seen, the foam designed to be an open-celled structure has very few closed cells. There also exists a geometric anisotropy, where parallel to the rise direction, the cells appear circular and perpendicular to the rise direction the cells appear elliptical with the major axis aligned along the rise direction. Since it has been shown that the physical properties vary depending on the loading direction, all foams were loaded parallel to the rise direction for consistency<sup>1</sup>. It was also observed, however, that the

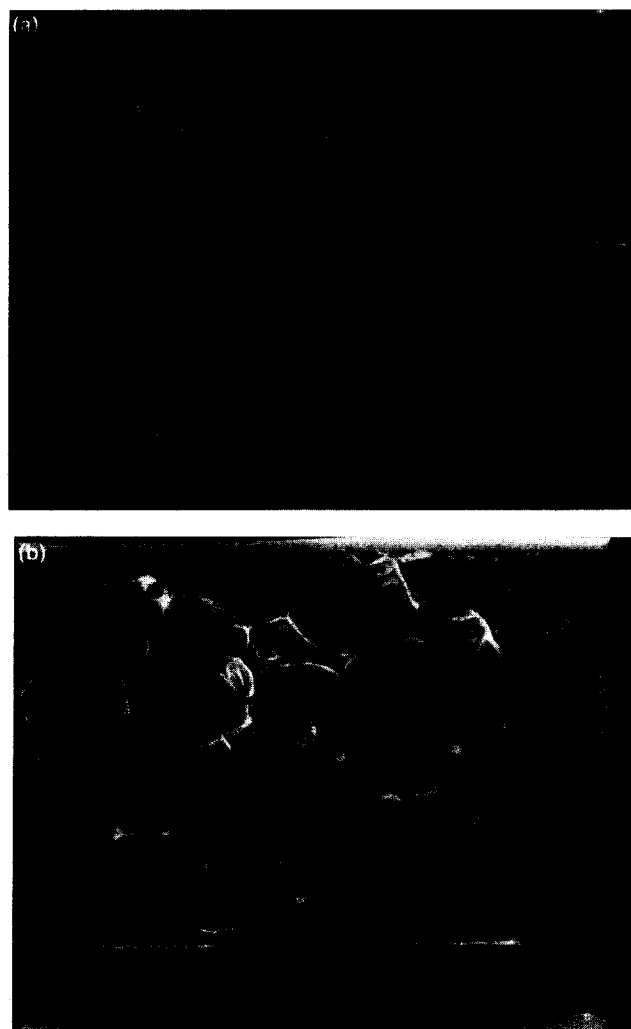


Figure 2 Scanning electron micrographs of slabstock foam, Fs4, (a) parallel and (b) perpendicular to the rise direction (bar = 1 mm)

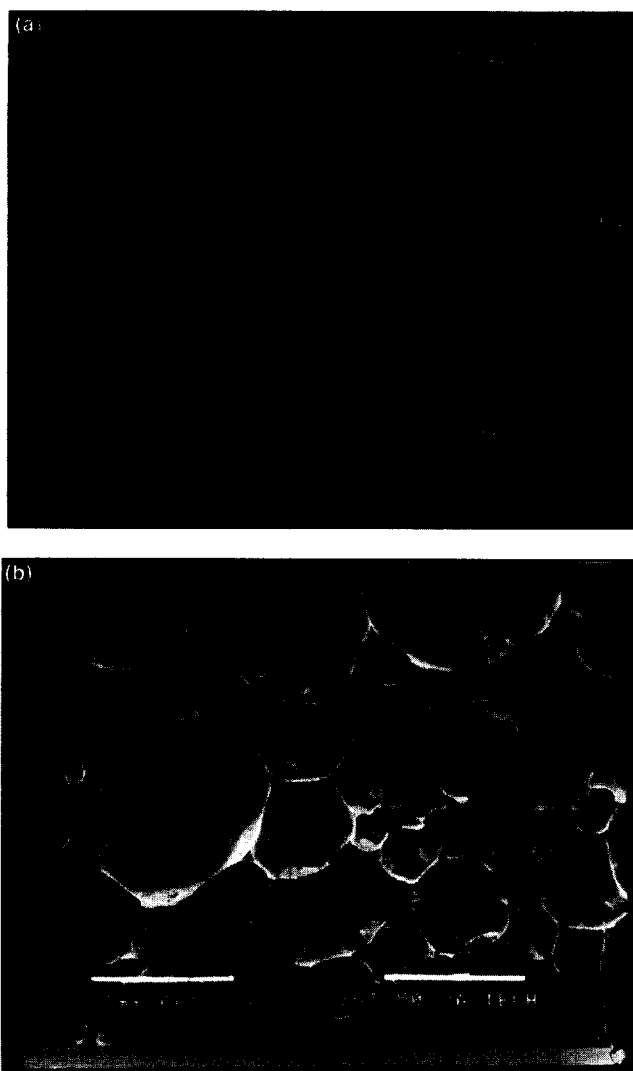


Figure 3 SEM of moulded foam, Fm4, (a) parallel and (b) perpendicular to the rise direction (bar = 1 mm)

time-dependent properties were independent of loading direction. Comparing these micrographs to those of the moulded foam, Fm4, shown in Figure 3a and b, it can be seen that the moulded foam, although also open celled, has somewhat more closed cells which can inherently alter the foam properties, e.g., air flow. For example, the airflow measurements of these two foams were  $5 \text{ ft}^3 \text{ min}^{-1}$  for Fs4 and  $1 \text{ ft}^3 \text{ min}^{-1}$  for Fm4 confirming that foam Fs4 does indeed have a greater cell openness. The cell struts are also much thicker thereby giving rise to a somewhat higher density foam. The geometric anisotropy observed in the slabstock foam is not evident in the moulded foam due to the reacting mixture being pressurized from all directions in the moulded foam.

#### Mechanical and viscoelastic behaviour

The compression set property of polyurethane foams used as load bearing materials may be the single most important property. Compression set was utilized to evaluate the foam morphology and network structure since it is sensitive to both. The compression set behaviour as a function of temperature and humidity of the moulded foams and slabstock foam is presented in Table 2. As the temperature or humidity was increased, the compression set also increased—especially with temperature. The amount of water in the formulation

Table 2 Percent set (CS) results

Condition	% CS Fm4	% CS Fm2	% CS Fs4
30°C–35%RH	2.5 ± 0.1	1.2 ± 0.2	
30°C–98%RH	9.5 ± 1.5	5.3 ± 0.3	
100°C–35%RH	59.0 ± 0.3	59.6 ± 0.6	
100°C–98%RH	64.3 ± 0.1	63.2 ± 0.1	15.2 ± 1.6
Day after CS	% CS Fm4	% CS Fs4	
0	63.2 ± 0.1	15.2 ± 1.6	
22		9.5 ± 1.0	
After 1 h @ 100°C		5.9 ± 0.3	
89	62.9 ± 0.1		
After 1 h @ 100°C	61.2 ± 0.2		

and thus hard segment content and density, appeared to have very little influence on the compression set. Comparing the compression set of the slabstock foam to the moulded foams show that at 100°C–98% RH the slabstock foam had considerably less set. The compression set for the slabstock foam was *ca.* 15% while for the moulded foams, it was *ca.* 63%. In addition, the slabstock foam displayed appreciable recovery. Over a period of 22 days at room temperature, this foam recovered to 9%. When subjected to 100°C for 1 h, this foam recovered even further to *ca.* 6%. *In great contrast, the moulded foam displayed no recovery.* These dramatic differences are clearly a result of differences in the solid morphology and/or covalent network content of the foams. The slabstock foam either has a better covalent network or better developed hard segment domains or both. This hypothesis will be explored later. It should also be pointed out that the incorporated copolymer polyol particles also contribute to the compression set of

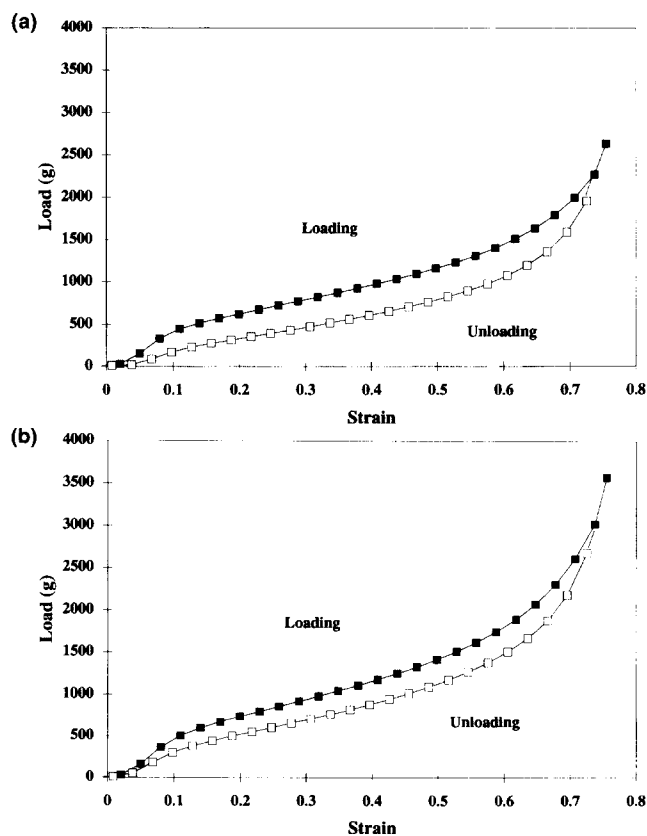


Figure 4 Compression load–strain behaviour illustrating both loading and unloading for moulded forms (a) Fm4 and (b) Fm2

the moulded foams—a topic that will be addressed in a separate publication now in preparation<sup>8</sup>.

The compression load–strain behaviour of the moulded foams is shown in *Figures 4a* and *b* where the loading and unloading curves are shown for each foam. As can be seen, the curves can be divided into three deformation regions as has been well described by Gibson and Ashby: the linear bending region, the elastic buckling region, and the densification region<sup>9</sup>. The first region is representative of elastic bending of the cell struts followed by a buckling of the cell struts where the strain increases with small changes in load. As can be seen, the final densification region begins at *ca.* 65% strain, the level of compression used for the load relaxation measurements. The area under both the loading and unloading curves was used to determine the energy of loading and unloading from which the

difference is used to quantify the amount of hysteresis. The results are given in *Table 3* which gives the percent hysteresis for each foam. Comparing *Figure 4a* to *Figure 4b*, shows that Fm4 displayed greater hysteresis than Fm2 as do the hysteresis values in *Table 3*. Since Fm4 does have a higher HS content, it also has a higher hydrogen bonding content which may be mechanically disrupted. The HS domains are believed to also act as stress concentrators thereby increasing the amount of localized stress leading to increased relaxation and hysteresis. *Figure 5a* illustrates the load–strain behaviour of a 2pph water content conventional slabstock foam and *Figure 5b* illustrates the load–strain behaviour of a 5pph water content foam, Fs5. As can be seen the general behaviour is the same as that of the moulded foams. The transitions from one deformation region to another occur roughly at the same levels of strain. The slabstock foam, however, displayed higher loads than the moulded foam of equal water content at any given level of strain. At a strain level of 60%, the load is *ca.* 2.5 kg for sample Fs2 and 2.0 kg for the moulded foam Fm2. As expected the densities of each are slightly different where the slabstock foam had a density of 2.85 lb ft<sup>3</sup> and the moulded foam a density of 3.3 lb ft<sup>3</sup>. Since the moulded foams density is greater, the lower loads observed for the moulded cannot be attributed to differences in density. As can be seen, the trend with water content is the same; increased water content resulted in greater hysteresis. More importantly, the amount of hysteresis is higher for this slabstock foam (Fs2) over that of the moulded counterpart (Fm2). Specifically, the hysteresis associated

**Table 3** First loading–unloading cycle hysteresis values

Foam	Hysteresis, %
Fm4	30
Fm2	23
Fs5	52
Fs2	30

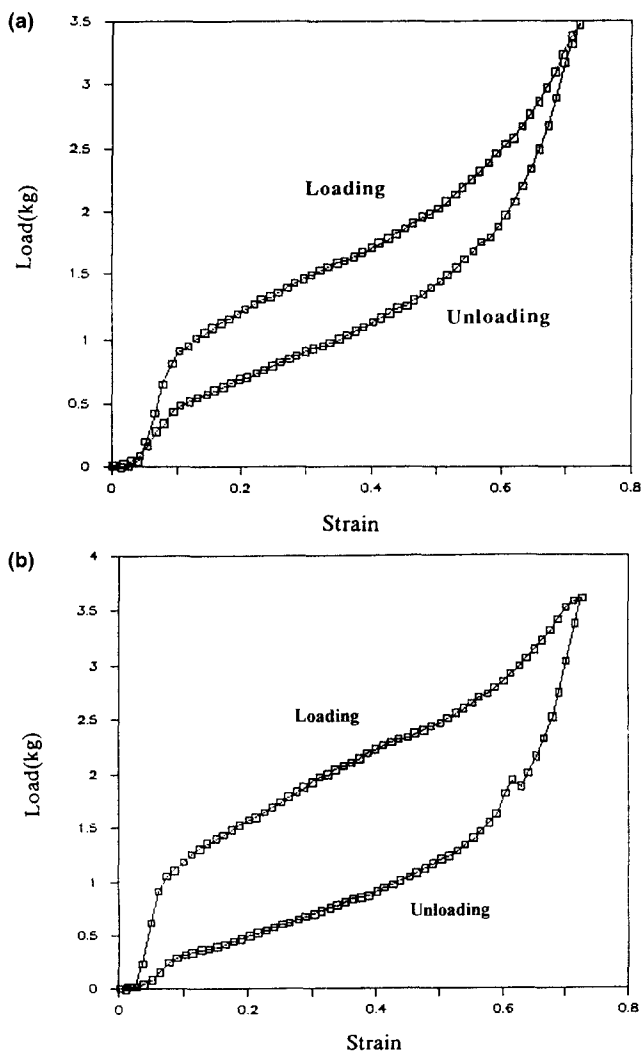


**Figure 5** Compression load–strain behaviour illustrating both loading and unloading for (a) Fs2 and (b) Fs5 (from ref. 1)

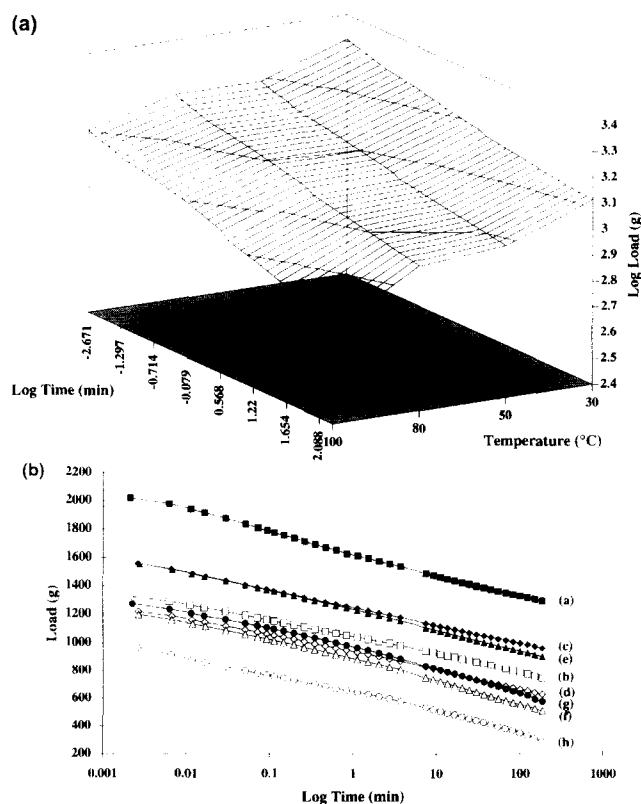


**Figure 6** Load relaxation behaviour for moulded foams Fm4 illustrated as a function of (a) temperature as well as (b) temperature and humidity. In (b) the letters designate the following conditions: (a) 30°C–35% RH, (b) 30°C–98% RH, (c) 50°C–35% RH, (d) 50°C–98% RH, (e) 80°C–35% RH, (f) 80°C–98% RH, (g) 100°C–35% RH, (h) 100°C–98% RH

with Fm2 was *ca.* 23% where that associated with Fs2 was 30%. The slabstock foam, as will be further discussed later, has better developed microphase separated hard segment domains, more hydrogen bonding and therefore even greater *localized* stress resulting in greater hysteresis.

The load relaxation behaviour was evaluated as a function of the temperature–humidity history and the formulation water content. This behaviour at constant 65% compression for Fm4 as a function of temperature is shown in *Figure 6a*. As can be seen, an increase in temperature systematically shifted the relaxation curves to lower loads and increased the amount of load decay. For example, the initial load decreased from 2019 g at 30°C–35% RH to 1271 g at 100°C–35% RH while the percent decay in a 3 h experiment increased from 36% to 54% for the two conditions respectively. In addition, the curve deviated from linearity at the highest temperature (100°C) relative to the observed behaviour at 30°C. The decrease in load and increase in percent decay with temperature is primarily due to hydrogen bond disruption occurring to a greater extent with temperature therefore increasing the amount of chain slippage that occurs. In addition, the increased soft segment mobility with temperature contributes to the increased percent decays and decreased initial loads. The nonlinearity observed at high temperatures, especially 100°C, suggests that the relaxation mechanism is dramatically enhanced. Here the amount of hydrogen bond disruption is dramatically increased. Retroreaction or reversal of the urethane reaction is also believed to occur at these high temperatures as was shown by Moreland *et al.*<sup>1</sup>. A

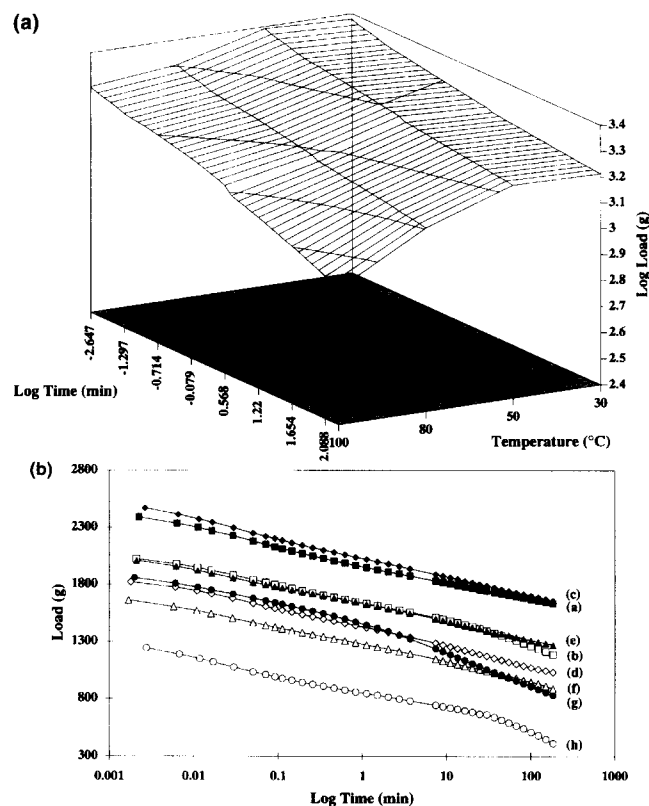


**Figure 7** Load relaxation behaviour for moulded foams Fm2 illustrated as a function of (a) temperature as well as (b) temperature and humidity. In (b) the letters designate the following conditions: (a) 30°C–35% RH, (b) 30°C–98% RH, (c) 50°C–35% RH, (d) 50°C–98% RH, (e) 80°C–35% RH, (f) 80°C–98% RH, (g) 100°C–35% RH, (h) 100°C–98% RH

similar trend was observed at 98% RH in the load relaxation behaviour. *Figure 6b* shows the effect of temperature and humidity on the load relaxation behaviour of Fm4. At a constant temperature an increase in humidity from 35% RH to 98% RH had a similar effect as did an increase in temperature from 30°C to 100°C at 35% RH. At 30°C, the initial load decreased from 2019 g at 35% RH to 1325 g at 98% RH. Thus, relative humidity as well as temperature ‘plasticized’ the system thereby promoting a greater time dependent behaviour.

The temperature dependence of the relaxation behaviour at a constant 35% RH for Fm2 is shown in *Figure 7a*. The exhibited behaviour was similar to that of Fm4. Foam Fm2, however, displayed higher loads—approximately 25% to 33% higher—a result of Fm2 having a higher density. Yet, the influence of temperature was similar, i.e. the relaxation curves decreased to lower loads with increasing temperature. The initial loads decreased from 2389 g at 30°C to 1860 g at 100°C. The percent decay at 30°C was 32% and at 100°C it was 56%. At temperatures above 80°C, the relaxation curves deviate from linearity relative to the observed behaviour at 30°C. Again this ‘plasticization’ has traditionally been attributed to the disruption of hydrogen bonds by temperature and/or humidity. Hydrogen bonding is reported to occur predominantly within the hard segment domains but can also occur among urea or urethane groups that interact with ether groups in the soft segment<sup>6,10</sup>.

*Figure 7b* illustrates both the influence of temperature and humidity on the load relaxation behaviour of moulded foam Fm2. The humidity effects are similar as with Fm4, where, at any temperature, an increase in humidity resulted in a significant ‘plasticization’ effect. Thus, increasing the humidity to 98% from 35% significantly enhanced the amount of load relaxation. As depicted in *Figure 7b*, at temperatures above 80°C, the relaxation curves deviate from linearity suggesting an enhancement of the mechanism resulting in accelerated relaxation. (Similar behaviour was also noted for the second moulded foam, Fm4.) The degree of ‘plasticization’ that occurs with temperature and humidity is evidence suggesting that the physical ‘cross-links’ play a significant role in the properties of the foam at ambient conditions. In addition, the size and perfection of the HS domains may be different in the moulded foams than slabstock foams which allows for more dramatic effects by temperature and humidity. This will be explored further in a later section.

Compared to slabstock foams of equal water content studied earlier by Moreland *et al.*, temperature and relative humidity alter the relaxation behaviour of the moulded foams more significantly (greater percent decays in the same 3 h experiment)<sup>1</sup>. The variable temperature load relaxation behaviour of a 2pph water content slabstock foam is shown in *Figure 8a*. Here, increasing the temperature actually resulted in an increase in the initial loads from 3000 g to 3500 g up to 100°C. In addition, the present decays decreased from 22% to 20%. At temperatures beyond 100°C, the initial loads significantly decreased and the percent decays significantly increased. Recall that moulded foam Fm2 not only displayed decreases in load with all increases in temperature but the percent decay also significantly increased. The observed increase in load with increasing temperature displayed by the slabstock foams was

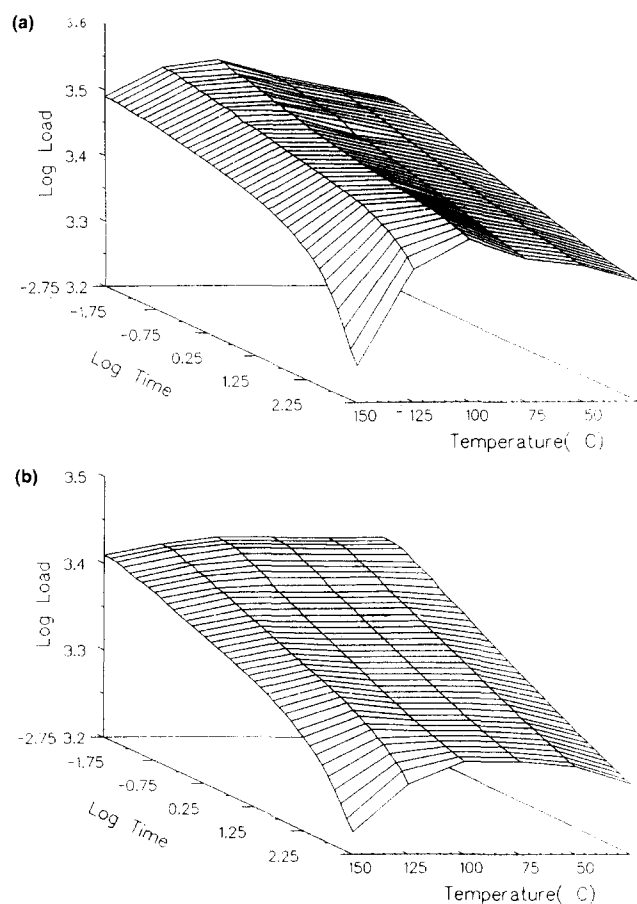


**Figure 8** Load relaxation behaviour illustrated as a function of temperature for slabstock foams (a) Fs2 and (b) Fs5 (from ref. 1)

attributed to an entropically driven elasticity effect of the rubbery covalent network. Thus, in the case where the HS content is low, the rubber elasticity effect overrides the softening of the HS domain. In addition, Moreland *et al.* observed that humidity had a relatively small effect on slabstock foams whereas for the moulded foams, this same variable dramatically softened them<sup>1</sup>. Again, the copolymer polyol particulates were shown to contribute to the time dependent response of the foams. The amount of decay increased by 30%–50% by their incorporation. As mentioned earlier, a separate publication will address the causes of this observation<sup>8</sup>.

The load relaxation of Fs5 is shown in *Figure 8b* which shows the influence of temperature on this 5 pph water content slabstock foam. While no increase in initial load was observed with increasing temperature, nor was a significant decrease noted. For example the initial load remained at *ca.* 2700 g from 30°C to 100°C beyond which the load decreased. Furthermore, the percent decay decreased for 30% at 30°C to 26% at 100°C beyond which the load increased considerably. Again, even for a high HS content foam, the observed behaviour was significantly different than that displayed by the high water content moulded foam. Recall that Fm4 displayed a strong sensitivity to temperature and humidity exhibiting a strong 'plasticization' trend with increases in either.

#### Morphological characterization

The foams covalent network was evaluated using solvent extraction studies in dimethyl formamide (DMF) to compare the level of cross-linking between

**Table 4** Extraction results for three of the foams studied

Foam	Sol fraction, %
Fm4	8.8 ± 0.1
Fm2	8.3 ± 0.2
Fs4	6.5 ± 0.5

the moulded foams and the slabstock foam and in part to account for the observed differences in the compression set behaviour and dramatic viscoelastic properties. The results presented in *Table 4* suggest that the amount of covalent cross-linking is slightly higher in the slabstock foam than the moulded foams as seen with the lower sol fraction for the slabstock foam. Between the two moulded foams, Fm2 appears to have a slightly lower amount of extractables than Fm4. However, this may be due to Fm4 having a higher amount of urea groups. Although it can be concluded that the level of covalent network is somewhat more developed in the slabstock foam, the dramatic differences in the compression set and viscoelastic properties were believed to arise in part from additional characteristics, and therefore further features of the foam morphologies were compared.

WAXS patterns were obtained to compare the amount of short range ordering within the HS of each foam that might make one system more labile than another at a given environmental condition. It should be recognized that while WAXS has been predominantly used to study crystalline polymers, it has also been used to evaluate the packing order in HS domains. Furthermore, the use of this technique is not intended to imply the existence of well-developed crystalline HS domains, since the high amount of the 2,4 TDI isomer certainly prevents this occurrence. The scattering pattern for the 4 pph water content slabstock foam is shown in *Figure 9a*. As can be seen, this pattern displays, in addition to an amorphous halo typical of liquid-like amorphous systems, a relatively sharp ring with an estimated Bragg spacing of approximately 4.5 Å and another outer but weaker ring with a spacing of *ca.* 6.0 Å. The exact origin of these rings is not yet confirmed absolutely but has been attributed to non-crystalline or para-crystalline hard segment ordering through hydrogen bonding<sup>11</sup>. The sharpness or diffuseness of these two rings can be used to qualitatively assess the level of ordering of the hard segments. The rings disappear with only the diffuse amorphous halo remaining after extraction in DMF (a solvent known to interact with urea) as displayed in *Figure 9b*. *Figure 10a* shows the WAXS pattern for Fm4 while *Figure 10b* shows the WAXS pattern for Fm2 both of which display *only* the amorphous halo suggesting that very little (if any) order exists amongst the TDI based hard segments and hence the HS domains of the moulded foams are more disordered than in slabstock foams. Thus, based on this lack of order, the moulded foams and their physical 'cross-links' allow for the easier 'plasticization' by heat and humidity thereby making them more labile than those in slabstock foams. This lack of structural order observed between the hard segments is believed to be both kinetic and thermodynamic based. Hard domain formation is very sensitive to the solubility of the urea segments in the polyol soft phase which is greater in moulded foams due to the stronger more favourable interactions between the hard segments and ethylene



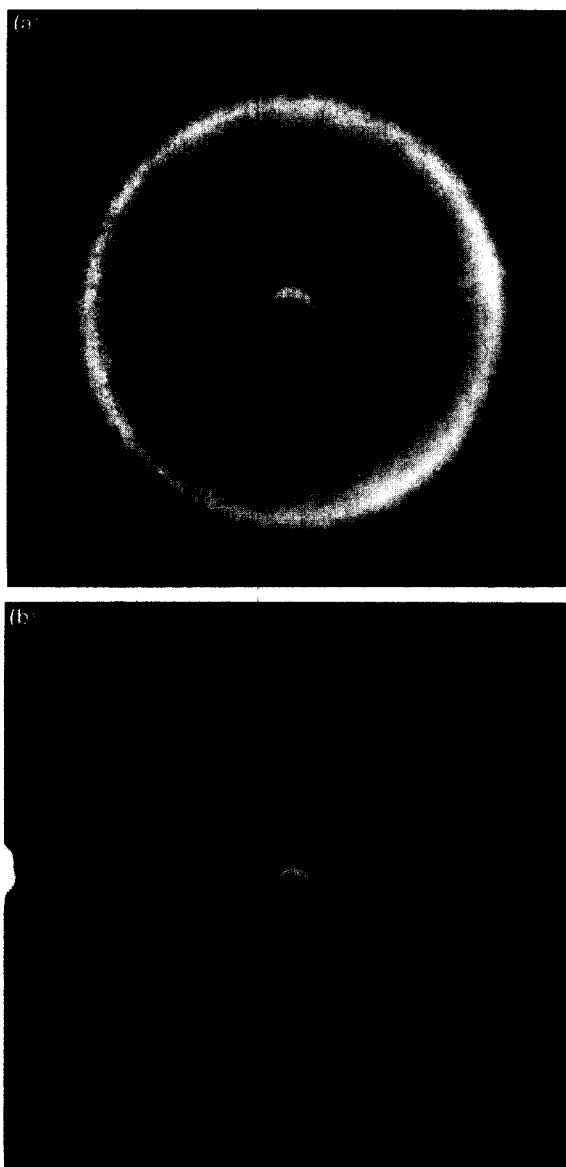


Figure 9 WAXS patterns of slabstock foams Fs4 (a) before extraction, and (b) after extraction

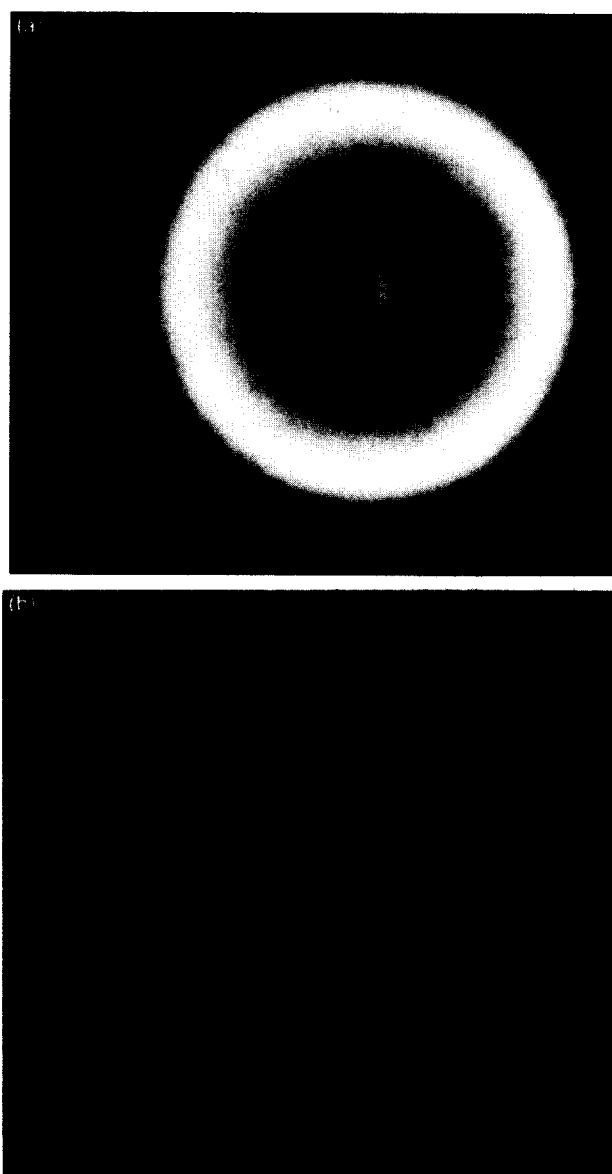


Figure 10 WAXS patterns of moulded foams (a) Fm4 and (b) Fm2

oxide capped soft segments (used to end cap the propylene oxide to decrease demould times in view of its higher reactivity). In addition, for bidentate hydrogen bonded urea to occur, it must principally develop prior to the gel point of the covalent network. Recall that diethanolamine is also added in the formulation of moulded foams to build softness, speed up gelation and decrease demould times. The rapid cross-linking that occurs early on in the network development makes it very difficult for the urea segments to associate (through diffusion) and to pack and form multiple bidentate hydrogen bonds with other hard segments thereby limiting perfection of the hard segment domain development.

To further verify the above evidence obtained by WAXS, FTi.r. analysis of the amide I region (carbonyl region) was studied which is shown for both moulded foams and the slabstock foam in Figure 11. The i.r. results show significant differences between the slabstock foam and the moulded foams. The slabstock foam displayed a strong bidentate absorption peak centred at  $1640\text{ cm}^{-1}$  which was non-existent in the moulded foams.

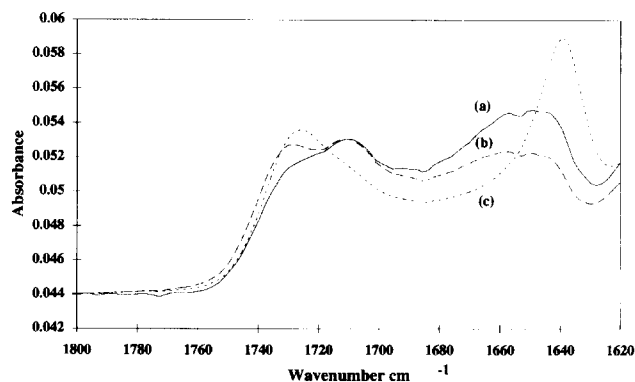


Figure 11 FTi.r. spectra for moulded foams (a) Fm4 and (b) Fm2 as well as slabstock foam (c) Fs4

This bidentate peak is indicative of hard segment ordering strongly supporting the WAXS results. Both moulded foams also displayed a moderate to strong monodentate absorbance centred at  $1700\text{--}1650\text{ cm}^{-1}$  as well as free urea centred at  $1715\text{ cm}^{-1}$ . Similar comparisons and observations have been reported by McClusky

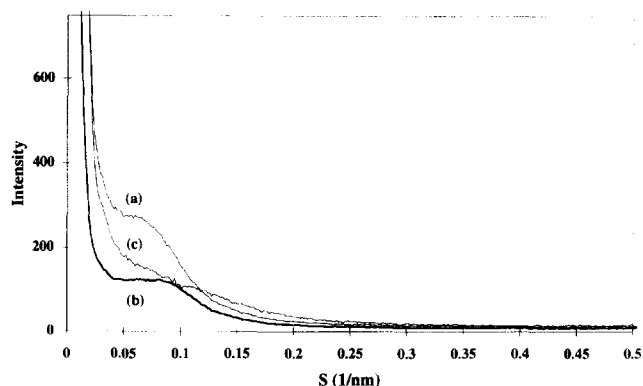


Figure 12 SAXS profiles of smeared intensity  $I(s)$  for the moulded foams, (a) Fm4, and (b) Fm2, and slabstock foam (c) Fs4

*et al.*<sup>6</sup>. For reasons mentioned above (specifically the addition of DEOA and EO capping in moulded foams), it is concluded that the moulded foams have a much more disordered physical network (hard segment domains) and covalent network which allows for greater 'plasticization' with temperature and humidity. Based on the WAXS and FTi.r. data, one might be misled into believing that the moulded foams are phase-mixed. For example, a homogeneous morphology would prevent hydrogen bonding between urea groups and packing in an orderly fashion. This might then lead to the trends observed in the WAXS and FTi.r. analysis of the moulded foams. To refute this, SAXS analysis was carried out and is shown in Figure 12 which is a plot of the normalized smeared intensity vs an angular variable. As can be seen, all samples display a shoulder (at *ca.*  $0.1 \text{ nm}^{-1}$ ) confirming that the samples are microphase separated on a scale of *ca.*  $100 \text{ \AA}$ . In fact, the shoulders associated with the moulded foams are more distinct. The three techniques of WAXS, SAXS and FTi.r. are crucial for obtaining a complete understanding of the localized foam morphology as has been shown. It can be concluded that while all systems are phase separated, the cohesiveness of the domains of the slabstock foams is much higher than that of the moulded foams.

## CONCLUSIONS

The viscoelastic and compression set behaviour of moulded foams varying in the formulation water/TDI content were studied and compared to those of conventional slabstock foams. It was found that systematic increases in temperature or humidity significantly deteriorated the moulded foams physical properties. These materials displayed great compression set especially at high temperatures and humidities. In addition, load relaxation results also showed the moulded foams to be extremely labile at elevated temperatures and/or humidities. In no case was an increase in the load with temperature observed such as that noted with respect to the slabstock foams. In view of these findings, the moulded foams were compared to conventional

slabstock foams in terms of structural and morphological features. Extraction studies were initially performed on both moulded and slabstock foams which showed that the level of covalent cross-linking was slightly higher in the slabstock foams. WAXS patterns of the slabstock foams displayed evidence of short range hard segment structural ordering which was not evident in either of the moulded foams. The i.r. results confirmed this by illustrating a strong urea bidentate absorbance in the slabstock profile while the moulded profiles only displayed monodentate and free urea absorbances. The structural and morphological as well as ensuing mechanical property variations are believed to arise from two major differences in the formulation components with the different processing techniques also having some influence. First, the use of ethylene oxide end capping in the moulded foams is also known to favour interactions with soft segment ether groups. Second is the addition of DEOA in the formulation with the intent again to decrease demould times taking advantage of the high functionality of DEOA thus allowing the foam to reach the gel point in shorter times. The early development of a network gel prior to the development of hard segment formation subsequently prevents the formation of highly ordered bidentate structures.

## ACKNOWLEDGEMENTS

This work has been financially supported by the Dow Chemical Company. Their support is gratefully acknowledged. Dr Randolph Grayson is also acknowledged for use of the transmission electron microscopy laboratory as well as Dr Eva Marand and Qingchun Hu for use of the Bio-Rad FTi.r. equipment.

## REFERENCES

1. Moreland, J. C., Wilkes, G. L. and Turner, R. B., *J. Appl. Polym. Sci.*, 1994, **52**, 549.
2. Herrington, R. M. and Klarfeld, D. L., *Proc. SPI-6th International Tech./Marketing Conf.*, 1983, p. 177.
3. Patten, W. and Seefried, C. G., *J. Cell. Plastics*, 1976, **12**, 41.
4. Skorpenske, R. G., Solis, R., Kuklies, R. A., Schrock, A. K. and Turner, R. B., *34th Annual Polyurethane Technical/Marketing Conference*, October 1992.
5. Thomas, O., Priester, Jr., R. D., Hinze, K. J. and Latham, D. D., *J. Polym. Sci., Part B: Polym. Phys.*, 1994, **32**, 2155.
6. McClusky, J. V., Priester, Jr., R. D., Willkomm, W. R., Capel, M. A. and Heaney, M. D., *Polyurethanes World Congress*, October 1993.
7. Skorpenske, R. G., Schrock, A. K. and Beal, G. E., *J. Cellular Plastics*, 1991, **27**, 560.
8. Dounis, D. V. and Wilkes, G. L., *The influence of Copolymer Polyols on the Viscoelastic Response of Molded Polyurethane Foams*, to be published.
9. Gibson, L. J. and Ashby, M. F., *Cellular Solids—Structure and Properties*, Pergamon Press, New York, 1988.
10. Paik Sung, C. S. and Schneider, N. S., *Macromolecules*, 1977, **10**, 452.
11. Armistead, J. P., Wilkes, G. L. and Turner, R. B., *J. Appl. Polym. Sci.*, 1988, **35**, 601.
12. Herrington, R. and Hock, K., *Flexible Polyurethane Foams*, Dow Chemical Co., Midland, MI, 1991.